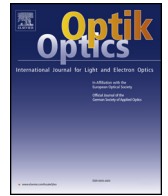




Contents lists available at ScienceDirect

Optik

journal homepage: www.elsevier.com/locate/ijleo

Original research article

Stiffness design of cantilevered structure with space optics load

Zhong-su Wang^{a,b}, Quan-feng Guo^a, Fan Jiang^{a,*}, Bo Chen^a, Qing-wen Wu^a,
Guo-qiang Wang^c^a Changchun Institute of Optics, Fine Mechanics and Physics, Chinese Academy of Sciences, Changchun, 130033, China^b University of Chinese Academy of Sciences, Beijing, 100049, China^c Jilin University, Changchun, 130011, China

ARTICLE INFO

Keywords:

Wide-angle aurora imager
Cantilever
Stiffness
Stiffened plate
Topological optimization
Finite element

ABSTRACT

Considering the low stiffness and strength for cantilever motor on the pitching shafting of a wide-angle aurora imager, a solution is proposed for setting up the motor-auxiliary-support, a stiffened plate, between the base and the motor. Firstly, the material, support position and structure form were determined. Secondly, the structural topology optimization was accomplished from the layout of stiffeners and the parameters of stiffeners by using the finite element simulation method. Then the structural design of the motor-auxiliary-support was determined. The simulation analysis and mechanical tests of the camera were carried out. It was found that the finite element analysis results were in agreement with the test results. After installed the motor-auxiliary-support, the frequency of the camera was increased by 14.58%, and the acceleration response of the sinusoidal vibration test on the motor was decreased by 79.32%. The structural ability to resist space mechanics environment had been improved significantly. The motor-auxiliary-support had a remarkable effect on improving the stiffness and strength of the structure.

1. Introduction

The wide-angle aurora imager is the main load of the FY3 (04) satellite. It is mounted on a three-axis stabilized satellite platform and flies along near-polar orbit, aiming at the detection imaging of far ultraviolet (FUV) radiation in the elliptical region of aurora. To achieve the imaging requirement of the entire polar region, the optical system is installed on a rotating pitch shafting, and the scanning range is from -60° to $+60^\circ$.

Considering the requirements of structural reliability, motor life, transmission accuracy and speed, the motor was placed at the outermost end of the pitching shafting. As a result, the axial dimension was longer on the side of the motor, the camera appeared eccentric and a large mass cantilever state. In the process of rocket launching, under the adverse mechanical environment such as vibration and impact, the cantilever motor may incur damage, owing to low stiffness and excessive response, which can lead to the failure of the motor or the inability of the pitch shafting. The scanning range could not be realized. Therefore, it is necessary to design the mechanical stiffness of the motor.

According to statistics, 30%–60% of satellite accidents are caused by vibration during launch and flight [1]. In the structural design of space camera, anti-vibration environment design is an indispensable. With regard to this paper, there are two schemes for stiffness design. One is to improve the rigidity of the camera. To do this, however, many structures must be changed. Moreover, the workload is large, the cycle is long, and the cost is excessive. Therefore, this approach is not suitable. The other approach consists of

* Corresponding author.

E-mail address: ghoethe@126.com (F. Jiang).

improving the local stiffness of the cantilever, eliminate the local vibration and reduce the mechanical response according to setting up the auxiliary support structure of the motor. The rods or thin plates support can be selected as the structure of the motor-auxiliary-support. The advantages of the rod support are its simple structure and convenient processing. However, the maximum external diameter of the rod cannot be greater than 8 mm, owing to the limitation of space size. According to structural simulation analysis, rod support had no significant effect on stiffness improvement. Therefore, the plate support was adopted. In order to essentially improve mechanical properties of structures, stiffeners of different types can be installed on the plate. Stiffened plates have been widely used in automotive, aerospace and civil engineering structures due to their high rigidity-to-weight ratio [2,3].

Numerous studies have been reported in open literature about stiffened plates. Bojczuk and Szteblelak [4] considered the layout and shape optimization of stiffeners in plates loaded in plane and in bending Kirchhoff's plates and studied the bending plates stiffened by ribs. Ali et al [5]. combined meshfree analysis and adaptive kriging for optimization of stiffened panels. Liu et al. [6] proposed a new Heaviside-function based directional growth topology parameterization (H-DGTP) of the casting constraints for simultaneously optimizing the layout and height of the stiffeners. Liu et al. [7] presented a parameter-free shape optimization method for the strength design of stiffeners on thin-walled structures. Li et al. [8,9] proposed a brand new optimizer to solve the structure layout design problems based on the so-called growth simulation, which learns from the clever morphology of leaf venation in nature. An et al. [10] proposed a two-level approximation method for multi-objective optimization of a composite stiffened panel. Chagraoui and Mohamed [11] proposed and applied a surrogate-based multidisciplinary design optimization (MDO) method on stiffened panels with several substructures and objectives. Bedair [12] presented some researches on stiffened plate structures and summarized some analysis and design methods for stiffened plate and shell structures. Mitra et al. [13] researched the large amplitude vibration problem of stiffened plates with free boundary.

In this study, the stiffness of the cantilever motor of the wide-angle aurora imager was designed and investigated. The optimization design of the motor-auxiliary-support was completed. Then, simulation analysis and test verification were conducted. In Section 2, the camera structure form and design requirements were introduced. In Section 3, the detailed optimization design of the motor-auxiliary-support was completed. Structural design was carried out from material selection, support position determination and structural form. Topological optimization of the layout of stiffeners and stiffened plate parameters was completed by using finite element method. In Section 4, the stiffness and strength of the camera were simulation analysis. In Section 5, the mechanics tests of the camera were carried out. The paper concluded with a summary in Section 6.

2. Design requirements and Structural form of the camera

2.1. Key technical indexes

The key mechanical indexes of the camera are shown in Table 1.

2.2. Camera structure form

The camera, as shown in Fig. 1, is mainly composed of base, U-frame, pitching shafting, two independent lens components, motor, and motor seat.

The motor mass is 2.0 kg and accounting for 18.2% of the camera mass. Under the excitation of mechanical loads, energy was transmitted from the base to the motor through the U-frame, the pitching shafting and the motor-seat. The forced vibration response of the motor was the largest, owing to the height increased and the local stiffness of the motor weak. The motor got destroyed when the response was greater than the limited value.

3. Design of the motor-auxiliary-support

3.1. Material selection

The material selection should have the following properties [14]: (1) excellent structural stiffness and strength, (2) high thermal stability.

The materials of space support structure include an aluminum alloy, magnesium alloy, CFRP, titanium alloy etc. as listed in Table 2. The specific stiffness of the CFRP is the largest. However, its cost is high and the processing cycle is long. Moreover, the aluminum alloy, titanium alloy, and magnesium alloy have similar specific stiffness values. In this study, the aluminum alloy material

Table 1
Key mechanical indexes of the camera.

Number	Item	Parameter
1	Mass(kg)	≤ 11
2	Frequency(Hz)	≥ 100
3	Volume(mm)	$\leq 450 \times 300 \times 563$
4	Safety margin	> 0

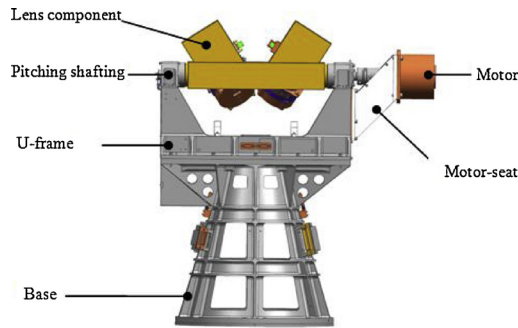


Fig. 1. Structural diagram of the camera.

Table 2
Material parameters of space support structure.

Material	Density ρ (g cm ⁻³)	Modulus E (Gpa)	E/ ρ (kJm /g)	Expansivity (10 ⁻⁶ K ⁻¹)	Conductivity λ (W.m ⁻¹ K ⁻¹)
Al alloy	2.71	69	25.5	23	155
TC4	4.44	110	24.7	8.8	5.4
Mg alloy	1.85	44.8	24.2	25.2	76
CFRP	1.56	140	89.7	0.3	35

was selected because of its workability, thermal conductivity and low cost.

3.2. Support position determination

Energy was transferred from the base to the motor via the U-frame and the pitching shafting when subjected to spatial mechanical loads. To reduce the response of the motor, one approach is to shorten the energy transfer path, and the other is to enhance the stiffness of the structure on the energy transfer path. It is the shortest transferring path when energy transmitted directly from the base to the motor. The most effective way to improve the stiffness is to set the support point in the suspension section. The closer the support position is to the motor, the higher is the supporting stiffness and the smaller is the mechanical response. Therefore, one support position of the motor-auxiliary-support was connected with the base, while the other support position was connected with the motor-seat and close to the motor mounting position as far as possible.

3.3. Structural form

3.3.1. Type selection of stiffened plate

For the base and the pitch shafting are rotary structures, the plate of the motor-auxiliary-support was selected as arc thin plate. In order to essentially improve mechanical properties of structures, stiffeners of different types can be used. In the case of bending plates, mostly stiffening ribs are applied [15]. A structure composed of a plate and stiffeners is called a stiffened plate. Stiffened plate is an effective way to improve structural overall stiffness. The static stiffness [16] includes the flexural stiffness, torsional stiffness, and compression stiffness, which reflects the structure’s ability to bear the static external load.

There are three types of stiffened plates: the well-type, the x-type, and the honeycomb-type. The stiffened plates’ type is shown in Fig. 2. According to the literature [17], the flexural stiffness is largest in the well-type stiffened plate, while the torsional stiffness is largest in the X-type stiffened plate. Compressive stiffness of three types of stiffened plate has little difference, and the well-shaped stiffened plate is slightly superior. Here, the well-type stiffened plate was selected for the motor-auxiliary-support.

3.3.2. Stiffeners layout

The design of the stiffened plate includes the introduction of a stiffener, determination of position and direction, and cross section

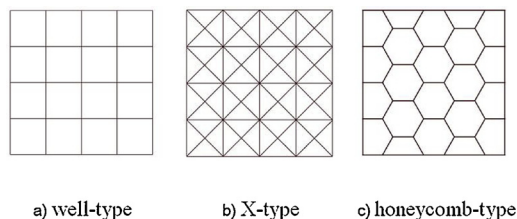


Fig. 2. Types of stiffened plate.

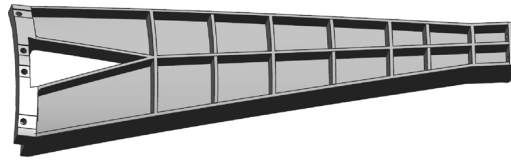


Fig. 3. Initial form of the motor-auxiliary-support.

size design [4]. It should be noted that the stiffener position and the optimal design of the cross section size are important considerations in the design of the stiffener [18].

The stiffeners layout was based on the ground structure method [19], according to the principle of maximum contribution [20] to the structural stiffness, excessive number of stiffeners were pre-established along the favorable direction, and then topology optimization method was used to determine stiffeners layout.

The initial form of the motor-auxiliary-support is shown in Fig. 3. The plate of the motor-auxiliary-support was an arc trapezoid plate that the side connecting the base was wide and the other side connecting the motor-seat was narrow. Eight stiffeners were arranged in the length direction and three stiffeners were arranged in the width direction of the plate. Width stiffeners were symmetrical to the width central axis of the plate. The initial parameters were as follows: plate thickness was 3 mm, stiffener height was 12 mm, and stiffener thickness was 5 mm.

3.4. Optimization of structure form

3.4.1. Stiffeners layout optimization

The layout of stiffeners directly affects the structural deformation, weight, natural frequency and stability. The essence of stiffener layout design can be considered as to find the optimal material distribution [21]. During the past decades, various methods based on topology optimization [22] have been developed to predict the optimal layout and/or sizes of the stiffeners for stiffened plate structures. Take the thickness of the plate [23] or the density [24,25] as design variables, and transform the problem of stiffeners layout design on the plate into the problem of the distribution of plate materials.

Stiffened plate is structural components consisting of plate reinforced by a system of stiffeners to enhance their load carrying capacities, as shown in Fig. 4. The main function of the plate is to absorb in-plane and vertical loads and distributes them to stiffeners, which can bear most of the vertical loads and ensure that the plate has enough stability to bear in-plane loads.

The bending control equations of the stiffened plate, the main flexural stiffness D_x and D_y , and the torsional stiffness H , are expressed as Eqs. (1) and (2):

$$D_x \frac{\partial^4 w}{\partial x^4} + D_y \frac{\partial^4 w}{\partial y^4} + 2H \frac{\partial^4 w}{\partial x^2 \partial y^2} = q(x, y) \tag{1}$$

$$\begin{cases} D_x = E^2 t / \{12 [1 - 1 + t^2 b / (h^3 a)]\} \\ D_y = EI / a \\ H = 2 [G^3 t / 12 + C / (2^a)] \end{cases} \tag{2}$$

where E and G are the elastic modulus and shear modulus, respectively; I is the inertia moment of the T-type cross section with a width of a ; c is the torsional stiffness of one stiffener; $q(x, y)$ is the distributed pressure load; w is the deflection; t is the plate thickness; h is the stiffener height; b is the stiffener thickness; a is the width of the stiffeners' layout. As expressed in Eq. (2), the stiffness of the stiffened plate is related to the plate thickness (t), the stiffener height (h), the stiffener thickness (b) and the width of the stiffeners' layout (a).

Weight savings in stiffened plate is an important design objective. It can have significant impact on the structure in terms of stiffness. The design of stiffened plate was intended for minimum mass and maximum first frequency. According to the actual form of the structure, the stiffeners in the width direction had little effect on the stiffness of the structure and the height of stiffeners was limited by the installation. Therefore, these two aspects were not as the main consideration of structural optimization. Optimization

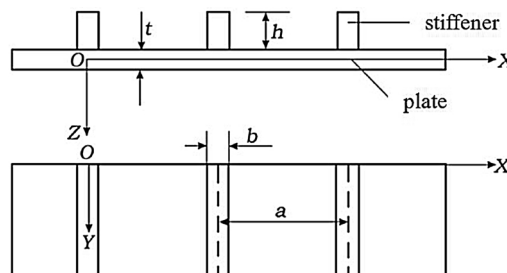


Fig. 4. Structure of stiffened plate.

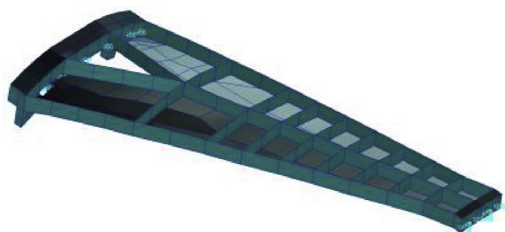


Fig. 5. Finite element model and constraint of the motor-auxiliary-support.

of the motor-auxiliary-support mainly focused on the arrangement of stiffeners in length direction and the thickness of the plate and stiffeners. The optimization problem of stiffened plate to solve, see Eq. (3), had for purpose to maximum the first frequency (f_1) while larger than 200 Hz, to less the mass(M) as possible of the studied plate.

$$s. t \begin{cases} Mass_{less}(X) \\ f_{1max}(X) \geq 200Hz \\ X \in \{a, b, t\} \end{cases} \tag{3}$$

The finite element simulation method was used for accomplishing structural topology optimization. The finite element model based on the structural model was generated by commercial software MSC-Patran and solved by MSC-Nastran. The shell element was selected for plate and stiffener and the body element was selected for connecting position with the base and the motor-seat. The boundary conditions are set in two places: the screw holes connected with the base and the motor-seat, respectively. Each node of screw holes was constrained by six degrees of freedom. The mesh and the boundary conditions of FE model is presented in Fig. 5.

Structural optimization was accomplished in two steps: Firstly, the layout of stiffener in length direction was optimized. Stiffeners which had little effect on the optimization objective were removed. Mass and first frequency of structure were calculated for different layout of stiffeners when the plate thickness, the stiffener thickness and the height were the initial design values. The results are shown in Table 3. Where, t is the plate thickness, h is the stiffener height, b is the stiffener thickness, M is the mass and f_1 is the first frequency of structure.

As shown in Table 3, with the decrease of the number of stiffeners, the mass decreased and the 1st frequency increased. Four stiffeners in length direction is taken for the structure.

Secondly, the parameters of stiffened plate, including the thickness of the plate and stiffeners, were optimized after the layout of stiffeners had been determined. Mass and first frequency of structure were calculated for different parameters of thickness of the plate (t) and the stiffener(b). The results are shown in Table 4. Where, t is the plate thickness, b is the stiffener thickness, M is the mass and f_1 is the first frequency.

According to the optimization results in Table 4, the structure performance is the best when the thicknesses of the plate and the stiffener are both 2 mm. At this time, the 1st frequency is 212.9 Hz and the mass is 0.508 kg. The final structural form of the motor-auxiliary-support is shown in Fig. 6. The 1st frequency diagram is shown in Fig. 7.

4. Simulation analysis of the camera

4.1. Establishment of finite element model

The finite element models of the camera without and with the motor-auxiliary-support, as shown in Fig. 8, were generated based on the solid models, and the constraint set at screw holes of the base connecting to the satellite platform. Each node of screw holes restricted six degrees of freedom.

Restricted at the screw hole of the base connecting to the satellite platform

4.2. Modal analysis

To investigate the stiffness contribution of the motor-auxiliary-support and the stiffness of the camera, modal analyses were carried out for the camera without and with the motor-auxiliary-support. The modes of X, Y and Z direction's analysis results are presented in Table 5. The vibration shape is shown in Fig. 9.

Table 3
The mass and 1 st frequency for different number of stiffeners.

t = 3(mm) b = 5(mm) h = 12(mm)						
number of stiffeners	8	7	6	5	4	3
M (kg)	0.916	0.888	0.876	0.857	0.839	0.822
f ₁ (Hz)	199.3	204.6	205.2	208.5	215.6	214.8

Table 4
The 1st frequency and mass for different thicknesses of plate and stiffener.

t (mm)	2				3			
	2	3	4	5	2	3	4	5
b (mm)	2	3	4	5	2	3	4	5
M (kg)	0.508	0.583	0.958	0.733	0.614	0.689	0.764	0.839
f ₁ (Hz)	212.9	219.2	222.16	223.5	197.3	205.7	210.6	213.6
t (mm)	4				5			
b (mm)	2	3	4	5	2	3	4	5
M (kg)	0.720	0.795	0.870	0.945	0.826	0.901	0.976	1.051
f ₁ (Hz)	186.9	196.1	201.8	205.7	180.3	189.4	195.6	199.9



Fig. 6. Final form of the motor-auxiliary-support.

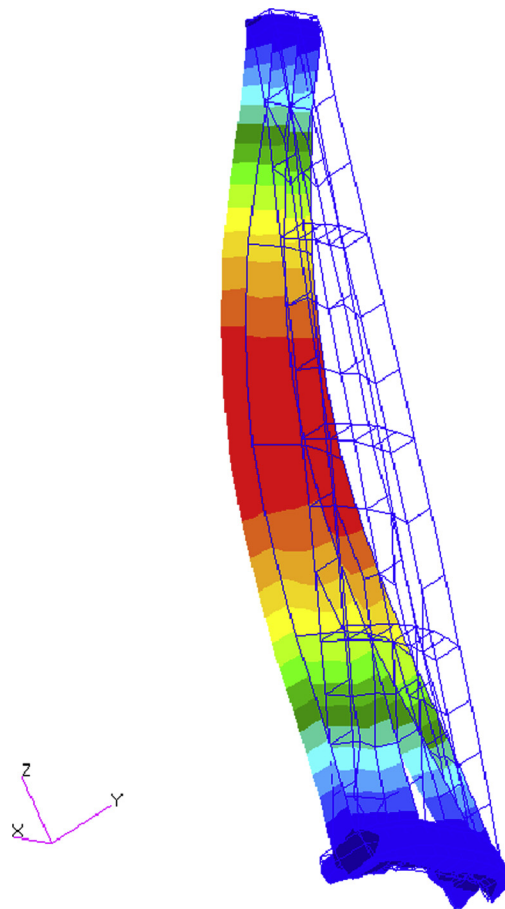


Fig. 7. The 1st frequency diagram.

As shown in Table 5, the X-direction mode of the camera increased from 96 Hz to 110 Hz after installed the motor-auxiliary-support, it increased by 14.58%. And as shown in Fig. 9, the local vibrations on the motor of the X-direction and Y-direction disappeared. These indicate that the motor-auxiliary-support was able to improve the structural stiffness.

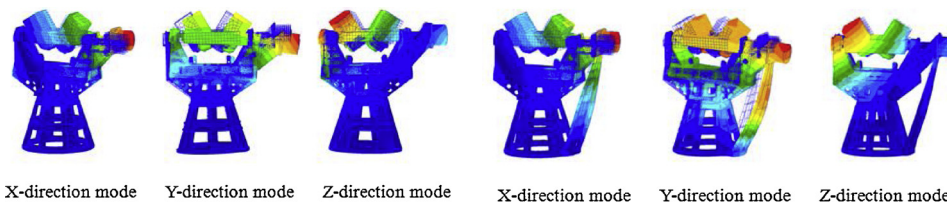


a) without the motor-auxiliary-support b) with the motor-auxiliary-support

Fig. 8. Finite element model and constraint of the camera.

Table 5
Model analysis results for the camera.

Direction	X	Y	Z
without the motor-auxiliary-support(Hz)	96	145	160
with the motor-auxiliary-support(Hz)	110	148	160
mode increase rate (%)	14.58	2.07	0



a) without the motor-auxiliary-support b) with the motor-auxiliary-support

Fig. 9. Vibration shape of the camera.

4.3. Sinusoidal load analysis

Investigating the supporting effect of the motor-auxiliary-support on the motor, sinusoidal load analysis of the camera was carried out. The simulation results of acceleration and stress responses on the motor are presented in Tables 6 and 7, respectively. With regard to the material safety margin, the safety factor was 1.3.

As shown in Table 6, the acceleration responses of X, Y, and Z-directions sinusoidal load obviously decreased after installed the motor-auxiliary-support. Moreover, the X-direction acceleration response decreased most significant, it reduced by 79.31%.

As shown in Table 7, the material safety margin(M.S) was $-0.84 (< 0)$ without the motor-auxiliary-support under X-direction sinusoidal load, which indicated that the structure was damaged and the structural strength must be enhanced. The material safety margins(M.S) of X, Y, and Z-directions increased significantly after installed the motor-auxiliary-support, and all of them were greater than zero, which satisfies the design requirements.

Table 6
Simulation results of acceleration response on the motor under sinusoidal load.

Load direction	acceleration (g)			acceleration magnification		
	X	Y	Z	X	Y	Z
without the motor-auxiliary-support	287.46	31.60	15.29	47.8	7.02	3.40
with the motor-auxiliary-support	59.43	10.4	8.08	9.91	1.39	1.08
acceleration decline rate (%)	79.31	67.09	47.16			

Table 7

The simulation results of stress on the motor under sinusoidal load.

Load direction		X	Y	Z
without the motor-auxiliary-support	stress (MPa)	2430	239	87.3
	safety margin (M.S.)	-0.84	1.58	4.32
with the motor-auxiliary-support	stress (MPa)	309	82.4	14.6
	safety margin (M.S.)	0.24	3.66	25.30

5. Vibration tests

5.1. Test state

To test the stiffness and the anti-space vibration environment capability of the camera, To investigate the supporting effect of the motor-auxiliary-support and to verify the correctness of the simulation analysis, mechanical tests of the camera with the motor-auxiliary-support were carried out. The test items included frequency sweep test and sinusoidal vibration test. The tests directions were X, Y and Z. The measuring acceleration sensor was set at the motor end face. The test state is shown in Fig. 10.

5.2. Frequency sweep test

To check the stiffness of the camera, the frequency sweep tests were carried out. The frequency ranged from 5 Hz to 200 Hz, the exciting load was 0.2 g and the scanning rate was 4oct/min. The test results are presented in Table 8.

As shown in Table 8, the fundamental frequencies of X, Y, and Z-direction were 112 Hz, 146 Hz, and 158 Hz, respectively. According to Tables 5 and 8, the results differences between the analytical and test were 1.78%, 1.37%, and 1.27%, respectively. It was found that the finite element analysis results are in agreement with the test results.

5.3. Sinusoidal vibration test

To test the anti-sinusoidal load capability of the camera and the supporting effect of the motor-auxiliary-support on the motor, the sinusoidal vibration tests of the camera were carried out. The test results are presented in Table 9 and the test curves are shown in Fig. 11.

As shown in Tables 6 and 9, the finite element analysis results were found to be in good agreement with the test results for acceleration responses on the motor under the sinusoidal vibration.

6. Conclusion

In this paper, a scheme of setting up the motor-auxiliary-support is proposed to solve the problems of low local stiffness and large mechanical excitation response for cantilever motor in pitch shafting of the wide-angle imager. The design of the motor-auxiliary-support was carried out from the aspects of material selection, support position and structure form determination. And the structural topology optimization was completed by using the method of finite element. The finite element simulation analyses for the camera with and without the motor-auxiliary-support were completed. The mechanical tests were carried out for the wide-angle imager with the motor-auxiliary-support. The simulation results were in good agreement with the test results. After installed the motor-auxiliary-support, the X-direction frequency of the camera increased from 96 Hz to 112 Hz, it increased by 14.53% and the acceleration response of the motor decreased by 79.32% under X-direction sinusoidal load. The effect of the motor-auxiliary-support on improving

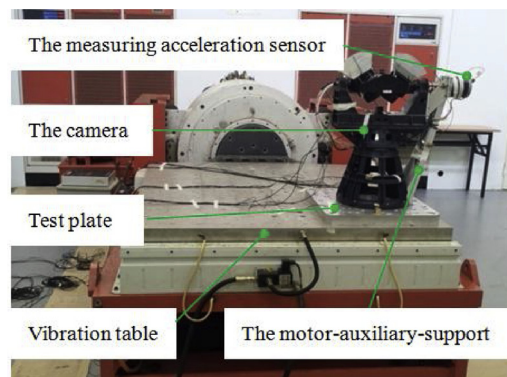


Fig. 10. Test state of the camera.

Table 8
Fundamental frequency of the camera.

Direction	X	Y	Z
Frequency(Hz)	112	146	158

Table 9
Responses of sinusoidal vibration tests on the motor.

Direction	X	Y	Z
Acceleration response (g)	52.3	9.2	8.1
Magnification	8.71	1.23	1.08

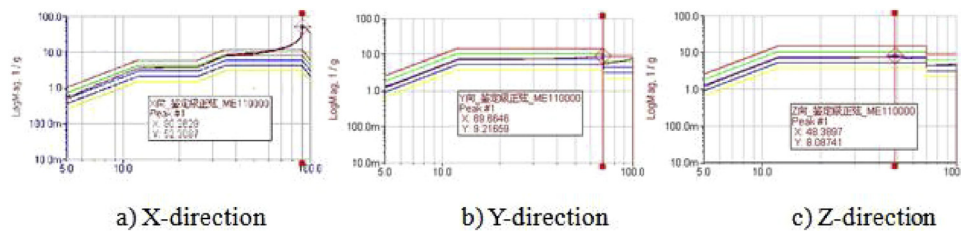


Fig. 11. Curves of sinusoidal vibration tests on the motor.

stiffness and strength were remarkable. This study is application oriented and may be a useful example of structural design for engineers.

References

- [1] Satellite Environmental Engineering and Simulation Test (II), Yuhang Publishing House, 1996.
- [2] S.M.B. Afonso, J. Sienz, F. Belblidia, Structural optimization strategies for simple and integrally stiffened panels and shells, *Eng. Comput.* 22 (2005) 429–452.
- [3] B. Chen, G. Liu, J. Kang, Y. Li, Design optimization of stiffened storage tank for spacecraft, *Struct. Multidiscipl. Optim.* 36 (2007) 83–92.
- [4] D. Bojczuk, W. Szeleblak, Optimization of layout and shape of stiffeners in 2D structures, *Comput. Struct.* 86 (13–14) (2008) 1436–1446.
- [5] A.Y. Tamijani, S.B. Mulani, R.K. Kapania, A framework combining meshfree analysis and adaptive kriging for optimization of stiffened panels, *Struct. Multidiscipl. Optim.* 49 (2014) 577–594.
- [6] Shutian Liu, Quhao Li, Wenjiong Chen, Hu Rui, Liyong Tong, H-DGTP—a Heaviside-function based directional growth topology parameterization for design optimization of stiffener layout and height of thin-walled structures, *Struct. Multidiscipl. Optim.* 52 (2015) 903–913.
- [7] Yang Liu, Masatoshi Shimoda, Yoji Shibutani, Parameter-free method for the shape optimization of stiffeners on thin-walled structures to minimize stress concentration, *J. Mech. Sci. Technol.* 29 (4) (2015) 1383–1390.
- [8] Baotong Li, Suna Yan, Qiyin Lin, Automated layout design of stiffened container structures based on the morphology of plant ramifications, *J. Bionic Eng.* 13 (2016) 344–354.
- [9] Baotong Li, Liuhua Ge, Jun Hong, An intelligent computational approach for design optimization of stiffened engineering structures, *Int. J. Precis. Eng. Manuf.* 18 (7) (2017) 1005–1012.
- [10] Haichao An, Shenyang Chen, Hai Huang, Multi-objective optimization of a composite stiffened panel for hybrid design of stiffener layout and laminate stacking sequence, *Struct. Multidiscipl. Optim.* 57 (2018) 1411–1426.
- [11] H. Chagraoui, M. Soula, Surrogate-based multidisciplinary design optimization for stiffened application, design and modeling of mechanical systems—III, *Lect. Notes Mech. Eng.* (2018) 147–156.
- [12] O.K. Bedair, Recent developments in modeling and design procedures of stiffened panels and shells, *Recent. Pat. Electr. Electron. Eng.* E 7 (3) (2013) 196–208.
- [13] A. Mitra, P. Sahoo, K. Saha, Large-amplitude dynamic analysis of stiffened panels with free edges, *J. Mech. Mater. Struct.* 6 (6) (2011) 883–914.
- [14] P.R. Yoder, *Opto. Mechanical System Design*, 2nd Edition, Marcel Dekker, 1993.
- [15] K. Inoue, M. Yamanaka, M. Kihara, Optimum stiffener layout for the reduction of vibration and noise of gearbox housing, *J. Mech. Des.* (2002) 124–518.
- [16] F.A.N. Q SH, *Engineering Mechanics*, Higher Education Press, Beijing, 2002.
- [17] D.W. Yu, W. Jiang, P.F. Feng, Static stiffness analysis and structure optimization of stiffened panel, *Mach. Design Manuf.* 2 (2) (2008) 4–6.
- [18] D. Wang, Z.H. Li, Layout optimization method for stiffeners of plate structure, *Chin. J. Comput. Mech.* 35 (2) (2018) 138–143.
- [19] K.S. Park, S.Y. Chang, S.K. Youn, Topology optimization of the primary mirror of a multi-spectral camera, *Struct. Multidiscipl. Optim.* 25 (2003) 46–53.
- [20] X.R. Ji, X.H. Ding, Design optimization method of stiffeners on plane and shell structures, *J. Mech. Strength* 34 (5) (2012) 692–698.
- [21] M.P. Bendsøe, N. Kikuchi, Generating optimal topologies in structural design using a homogenization method, *Comput. Methods Appl. Mech. Eng.* 2 (71) (1988) 197–224.
- [22] T.Y. Chen, C.B. Wang, Topological and sizing optimization of reinforced ribs for a machining centre, *Eng. Optim.* 40 (2008) 33–45.
- [23] Y. Huang, D.Y. Wang, Free vibration analysis of the stiffened panel, *Ship Eng.* 30 (6) (2008) 1–3.
- [24] S.M. Afonso, J. Sienz, F. Belblidia, Structural optimization strategies for simple and integrally stiffened panels and shells, *Eng. Comput.* (Swansea) 22 (4) (2005) 429–452.
- [25] Yang Liu, Masatoshi Shimoda, Non-parametric shape optimization method for natural vibration design of stiffened shells, *Comput. Struct.* 1 (146) (2015) 20–31.